Silicon (2021) 13:3003–3010
https://doi.org/10.1007/s12633-020-00649-1

ORIGINAL PAPER

Effect of SiO_2 Addition on Chromium Transitions in Borate Glasses

M. Farouk[1] · Dhia-Aldin Slibi[1] · Z. M. Abd El-Fattah[1] · M. Atallah[2] · M. A. El-Sherbiny[1] · Moukhtar A. Hassan[1]

Received: 21 April 2020 / Accepted: 11 August 2020 / Published online: 18 August 2020

Abstract
Melt-quenching technique was used to prepare borosilicate glasses of composition $xSiO_2$- (75-x) B_2O_3–24.7Li_2O-0.3Cr_2O_3 (x = 0, 10, 20, 30, 40 and 50 mol%). With increasing the former content, both Cr^{6+} and Cr^{3+} optical transitions undergo strong intensity variations. The crystal field strength (10Dq) is increased, while Racah parameters (C,B) are decreased with increasing SiO_2 content. The ratio estimated Dq/B values confirmed a weak crystal field environment for Cr^{3+}ions, and further suggest a more covalent bond character. The ESR results revealed that Si-contained samples exhibit a strong microwave absorption signal, and justified the presence of both Cr^{3+} and Cr^{6+}(charge transfer into $3d^0$ $2p^{6+} = 3d^1Cr^{5+}$) oxidation states. The fingerprints of borate and silicate relevant structural groups were clearly identified from FTIR spectroscopy.

Keywords Borosilicate glasses · Chromium hexa/trivalent · Ligand field theory · ESR spectra · FTIR

1 Introduction

Glasses doped with transition metal (TM) oxides are interesting materials for several potential applications, due to their technologically unique properties and commercial availability. For example, these glasses could be integrated as active components in diverse optical, electrical, thermal, and mechanical devices [1–7]. Furthermore, TM ions play a central role nowadays in probing glass and/or crystalline structures, since they own outer *d*-orbitals of broad radial distribution responsible for their superior sensitivity to minute changes in the surrounding actions [8–11]. Additionally, materials having multivalence states, such as Cr for instance, are convenient as cathode elements in rechargeable batteries, since they also offer high energy density and capacitance [12, 13].

Among several transition metals, Cr^{3+} ions are commonly used as activators in different luminescence materials and to color glasses, particularly when introduced in small quantities in the glass matrix, beside their large influence over other relevant physical properties such as the insulating strength of the glass samples [12–17]. Furthermore, Cr^{3+}ions in $3d^3$ configurations have excellent VIS–NIR broadband luminescence, laser performance (suitability for solid state lasers) and applications in solar collectors [1, 2, 6, 18, 19]. The special glass characteristics, such as high glass forming ability, lower glass transition temperature, high thermal stability, and transmission, could be utilized by using alkali ions in varying types and quantities. In this context, Li_2O ions turn out to be of particular interest given their smallest ionic radius compared to other alkali ions, which have shown to enhance photoluminescence in colored glasses [20]. Moreover, the addition of SiO_2 to alkali borate glasses is known to enhance its durability, hardness, and the transmission to UV light [21]. Hence the mixed former alkali-borosilicate glasses offer promising host to accommodate different modifying oxides and ions from transition metal oxides (TMO), such as Cr_2O_3. Although alkali borate glasses are highly transparent to visible light, their strong optical absorption in ultraviolet UV region significantly mask relevant high energy optical transitions [17]. Furthermore, the availability of boron in both BO_3 and BO_4 structural units and the strong B-O covalent bonds render borates glasses highly stable [22]. Chromium ions normally participate in glass networks with CrO_4 (Cr^{6+}), CrO_6 (Cr^{3+}) and to lesser extent with CrO_3 structural units [21, 23]. Among varies oxidation states (e.g., Cr^{2+}, Cr^{3+}, Cr^{5+}or Cr^{6+}) chromium ions are most frequently found in two

✉ M. Farouk
mf_egypt22375@yahoo.com; m_farouk@azhar.edu.eg

✉ Moukhtar A. Hassan
moukhtar_hassan@yahoo.com; m.a.hassan@azhar.edu.eg

[1] Physics Department, Faculty of Science, Al-Azhar University, Cairo 11884, Egypt

[2] Basic Science Department, Higher Technological Institute, 10th of Ramadan City, Egypt

valence states. These are Cr^{3+}, which together with CrO_6 structural units act as modifiers, and Cr^{6+} acting as network formers with CrO_4. Glasses doped with Cr^{3+} and Cr^{6+} ions revealed distinct colors which can be observed by UV-VIS spectroscopy [18, 24]. In the present study, lithium borosilicate glasses doped with Cr_2O_3 were prepared. These glasses were characterized by FTIR, UV–VIS Optical absorption. The latter allowed the extraction of ligand filed parameters (Dq, Racah interelectronic repulsion parameters, B and C). Additionally, the electron spin resonance (ESR) was used to shed the light into the different Cr oxidation states.

2 Experimental Setup

Following the melt quenching technique, the glass compositions $xSiO_2$- (75-x) B_2O_3–24.7Li_2O-0.3Cr_2O_3(x = 0, 10, 20, 30, 40and 50 mol%) were prepared. The mixtures were ground together in an agate mortar and transferred into a porcelain crucible. The batches were melted in an electrical furnace under ordinary atmospheric conditions, in the temperature between 1100 and 1200 °C for one hour until a bubble free liquid was formed. The molten were quenched rapidly to room temperature between two polished copper plates. Green colored glasses with high optical quality and transparency were obtained. The amorphous nature of the prepared glasses was ensured from X-ray diffraction (XRD) measurements, performed using XRD-6000 Shimadzu X-ray diffractometer, with a Cu Kα radiation of wavelength λ = 1.54 Å for an angular range between 5 and 80°. Optical absorption spectra of the samples were recorded using JenWay-6405-type UV-VIS spectrophotometer in 190 to 1000 nm spectral range. Electron spin resonance (ESR) data were collected using EMX Bruker-type spectrometer, operating at the X-band frequency with 100 kHz field modulation and 10 mW microwave power. The magnetic field was varied between 75 to 6000 G. For reasonable quantitative spin analysis, the weight of the powder is kept fixed for all samples. Infrared absorption spectra were recorded in the range 400–1600 cm^{-1} using FTIR Nicolet 6700 spectrometer, on powdered samples pressed into disks after mixing with high purity KBr.

3 Results and Discussion

3.1 X-Ray Diffraction

Figure 1 shows X-ray diffraction (XRD) patterns for Si = 0, 30 and 50 mol% samples, taken as representative examples. The spectra exhibit no traces of crystalline phases, i.e., no continuous or discrete sharp peaks, but rather the amorphous characteristic broad hump at 2θ ~ 23°, which is a typical feature of borate glasses. The absence of well-defined diffraction peaks rules out the occurrence of long-range atomic arrangement and, therefore, clearly confirms the glassy nature of the samples [25–30]. The second weak halo around 2θ ~ 45°, which is better defined for the SiO_2-free sample, is commonly associated to the phase separation character of borate glasses [30].

The intensity of XRD hump at 2θ ~ 23° was found to decrease with the amount of Silicon oxide, with an incremental broadening of the hump, reflecting an enhanced amorphous character of the prepared samples and substantial loss of the short-range order [31, 32]. This behavior is quantified in the inset of Fig. 1, by depicting the variation of the area under the hump, obtained from a standard Gaussian fitting, with the SiO_2 content.

3.2 Optical Properties

Figure 1 shows the optical absorption spectra of all glass samples taken at room temperature. An overall shift of the absorption edge of ~0.1 eV towards lower wavelengths (i.e., blue shift) was observed while increasing the SiO_2 content. Additional spectral features related to discrete Cr transitions were observed, the identification of which calls for a detailed deconvolution process for all glass samples, as exemplified at the inset of Fig. 2. Specifically, the spectra exhibited strong absorption bands at ~338 and ~ 370 nm which are characteristic for chromium ions in Cr^{6+} oxidation state, and are attributed to $^4A_{2g}\rightarrow{}^4T_{1g}$ and $^4A_{2g}\rightarrow{}^2A_{1g}$ optical transitions, respectively [1–5, 24, 33]. These bands undergo spectral sharpening and intensity enhancement with SiO_2 contents, as shown Fig. 2. Additionally, they were found to shift to higher wavelength (338–348 nm and 370–390 nm) with increasing the silicate oxide content. The origin of the two UV bands assigned to Cr^{6+} oxidation state, stems from charge transfer with p levels [1–3, 34, 35], which in the presence of crystal field splits into two states that show up as two optical transitions in the visible and UV spectral regimes [1–3, 34–36].

Indeed, optical transitions in the visible regime within the transparent glass host is responsible for the glass color. Two such bands are located at ~421 and ~ 619 nm as shown in Fig. 2, which are resulting from d-d transitions of Cr^{3+}ions (d^3) in octahedral symmetry glass environment (strength of crystal field and covalency), and are assigned to $^4A_{2g}\rightarrow{}^4T_{1g}$ and$^4A_{2g}\rightarrow{}^4T_{2g}$ transitions, respectively [1–3, 34–37]. Additionally, the spectra contain a weak fine structure in the form of spectral dips at ~770 nm. These faint Fano anti-resonances dips are present because of the of spin-orbit interaction and the level mixing between ^2E and ^4T and $^2T_1$ and $^4T_2$ [1–3, 34–38]. Contrary, the band located at ~421 nm predominantly defines the yellowish color of the glass, while the ~619 nm band contributes to the greenish color [1–3, 18]. The intensity of the absorption bands at ~421 and 619 nm increases with increasing SiO_2 content. This trend is fully supported by the observed glass color transformation from dark-

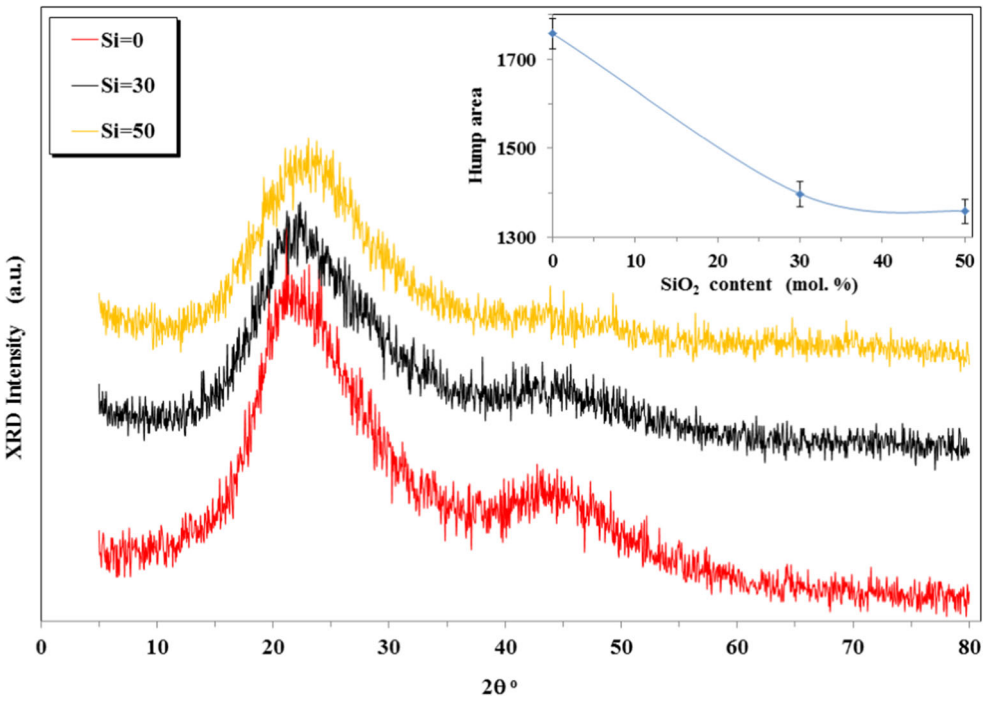

Fig. 1 XRD patterns for $x = 0$, 30 and 50 mol% samples of composition $x SiO_2$- (75-x) B_2O_3–24.7Li_2O-0.3Cr_2O_3. The inset depicts the variation of the area under the spectral hump with the composition

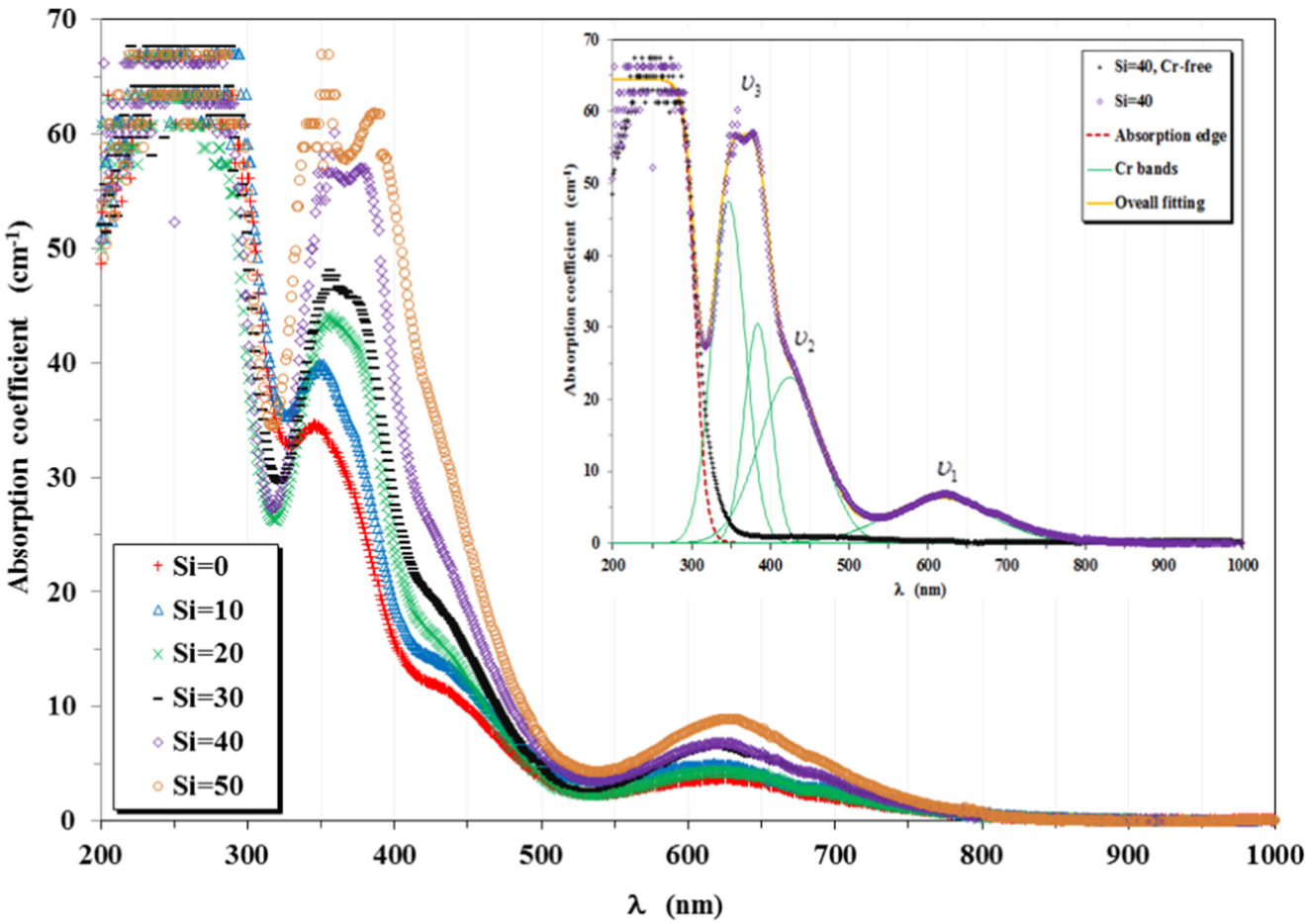

Fig. 2 Optical absorption spectra for all investigated samples of composition $x SiO_2$- (75-x) B_2O_3–24.7Li_2O-0.3Cr_2O_3 and the inset is Si = 40 and Cr-free Si = 40 samples. Brown, green and orange curves are the deconvolution results from the Si = 40 sample

green towards yellow-green with SiO_2 content. The two absorption bands at 421 and 619 nm are shifted to higher wavelength (i.e., red shift) with increasing SiO_2 content.

The optical absorption spectra presented in Fig. 2 provide additional information regarding the interactions within the host, such as the crystal field strength (10Dq). The band located at ~619 (υ_1) defines the magnitude of 10Dq [1–3, 16, 25, 37];

$$10Dq = v_1 \tag{1}$$

The Racah parameters B &C defining the inter-electron Coulomb repulsion between 3d electrons of Cr^{3+}ions, are obtained following the equations [1–3, 15, 33]:

$$B = \frac{(2v_1 - v_2)(v_2 - v_1)}{(27v_1 - 15v_2)} \tag{2}$$

$$C = \frac{v_3 - 4B - v_1}{3} \tag{3}$$

where$v_2$refers to the band positioned at ~421 nm and v_3 is the position of Cr^{6+} band at the average sum of 337 and 369 nm bands. By substituting v_1, v_2 and v_3, in (cm^{-1}) energy units, obtained from the deconvolution process, into Eqs. (1), (2), (3), the 10Dq, B and C ligand field parameters were obtained and presented in Fig. 3 (a,b). The 10Dq and (B, C) parameters clearly follow an opposite behavior with SiO_2 content, reflecting a relatively weaker inter-electronic repulsion within d-shell. Consequently, the chemical bonds between the ligands and Cr^{3+} ions acquire more ionic character [1–3, 19, 38]. This may be illustrated by the slightly longer Cr–O distances in glass materials than oxide crystals [6]. The values of B are much lower than B = 1030 cm^{-1}, i.e., the value of the free Cr^{3+} ion [7]. It is well-established that the relation between Racah parameters is C ≈ 3.6 B, which is reasonably satisfied for the present system as listed in Table 1. Similarly, the ratio Dq/B defines the strength of the ligand field, where Dq/B less or greater than 2.3 indicates the weak or strong crystal field, respectively. In the present studied glass, the ratio of Dq/B changes from 1.99 to 2.17 with increasing of SiO_2 content [1–3, 10, 39, 40]. This indicates that Cr^{3+}ions are in the weak crystal field regime, and further suggests more covalent bond character for this glass system [17, 33]. This can be supported by estimating the bonding formation (the nephelauxetic, h) of the ligand encoded within Racah parameter B as [1–3, 8, 25]:

$$h = \frac{\left[\left(B_{free} - B\right)/B_{free}\right]}{K_{cr^{3+}}} \tag{4}$$

where, B_{free} is Racah parameter for the free (gaseous) Cr^{3+} ion and k is the central Cr^{3+}ion, which take the values B_{free} = 918 cm^{-1} and K_{Cr3+} = 0:21 [1–3, 36, 38]. Therefore, for all glass samples, B is lower than B_{free}, as given in Table 1. The calculated nephelauxetic h parameter is increased with SiO_2content, indicating a gradual increase in the covalent environment of Cr^{3+} as well as increased d-electrons localization [24, 26, 38].

The measurement of the overall absorption edge is a useful average method for the investigation of the momentum-integrated electronic structure in crystalline and amorphous/glassy materials [39]. The absorption coefficient (α) stands as the main factor in estimating the $(\alpha h\nu)^{0.5}$ and ln(α) parameters for large and low absorption, respectively. The optical band gap (E_g) can be estimated according to the equation [1–3, 41]:

$$\alpha h\nu = A\left(h\nu - E_g\right)^n \tag{5}$$

The best fit to the optical absorption edge was obtained for $n = 2$, which indicates allowed indirect band transition for the glass samples. The values of E_g as obtained from this fitting for all investigated samples are given in the Table 1. With increasing SiO_2 contents, the optical band gap is enlarged consistent with the reduced number of NBO's suggested later from FTIR results. On the other hand, the reduced number of non-bridging oxygens and the rigidity reduce the degree of localized states within the glass network resulting in wider band gap and shifting the absorption edge towards lower wavelength [21, 25]. Fluctuations of the gap energy within ~0.1 eV was obtained for this glass system with average value of 3.68 ± 0.05 eV. In fact, the higher amorphous degree reported from XRD data for SiO_2 contained samples, which signals reduced band gap size, compensates the large gap induced by NBO's, so that the final gap size is only partially (± 0.05 eV) changed with SiO_2 additives.

Table 1 The estimated band gap energy, ligand field parameters (C/B, Dq/B), and the bond formation parameter(h) as a function of SiO_2 content

SiO_2 content (mol. %)	Band gap energy	Ligand field parameters		
	E_g (eV)	C/B	Dq/B	*h*
0	3.63	3.62	1.99	0.54
10	3.63	3.59	2.05	0.65
20	3.73	3.57	2.10	0.74
30	3.70	3.57	2.13	0.80
40	3.74	3.53	2.15	0.83
50	3.72	3.51	2.17	0.87

3.3 ESR Spectral Studies

The room temperature ESR spectra for x = 0, 20 and 40 mol% samples doped with fixed 0.3 mol% Cr_2O_3 are shown in Fig. 4. It is observed that all Cr characteristic resonances lose intensity with increasing SiO_2 content. The ESR spectra

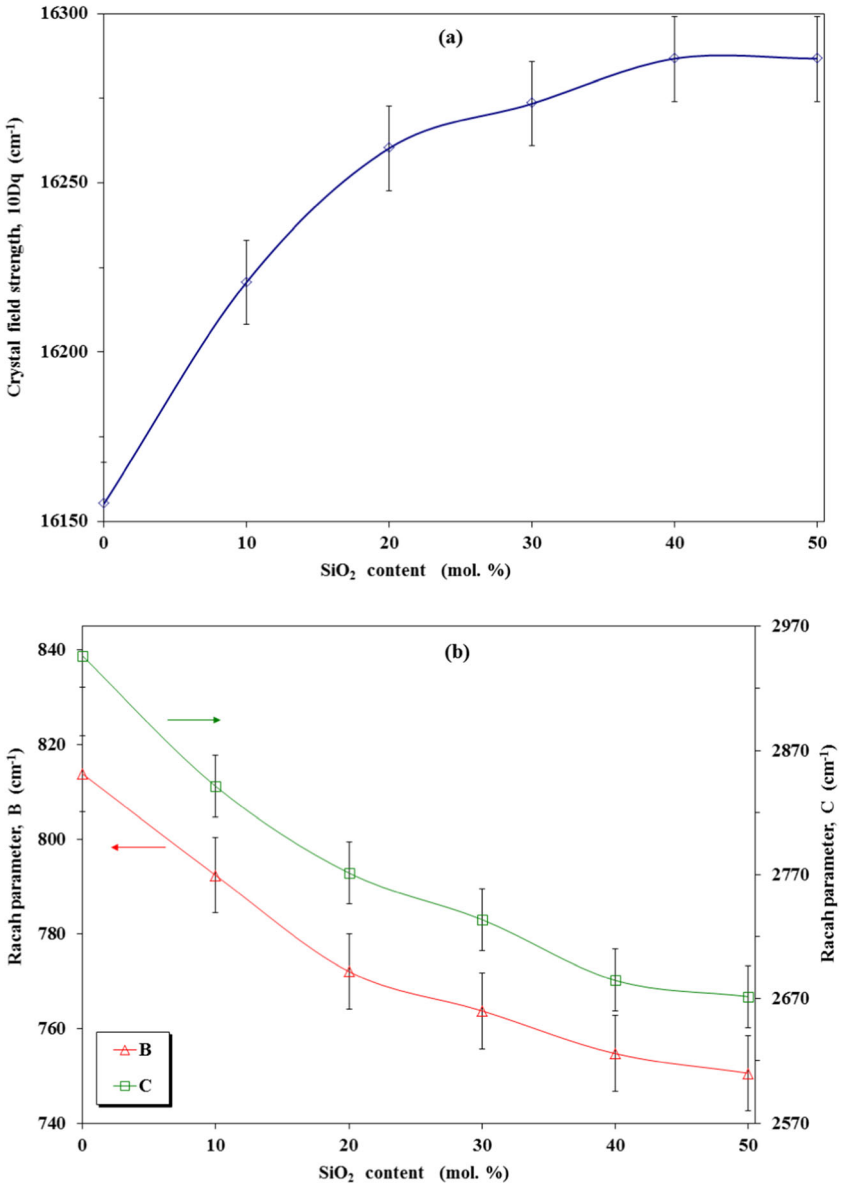

Fig. 3 Ligand field parameters composition dependence; (**a**) crystal field strength (10Dq), and (**b**) Racah parameters (B,C)

exhibit resonances with effective g values at 4.82 (1430 G), 4.08 (1688 G), 2.25 (3061 G) and 1.93 (3571 G), where G refers to the magnetic field in Gauss units. The first resonance at ~1430 G confirms the presence of isolated Cr^{3+} ions subject to strong crystal field in distorted octahedral configuration [1, 2, 9, 13, 17, 24, 42, 43]. The second strong absorption at ~1688 G has its origin in Cr^{3+}ions [1, 2, 44, 45]. The magnetic resonance of these glasses arises from the $3d^3$ electron in paramagnetic Cr^{3+}ions (The Cr^{3+} free ions have $3d^3$ electrons and $^4F_{3/2}$ ground state). Similar to optical absorption spectra, the Cr^{3+}ions ground state in an octahedral crystal field is $^4A_{2g}$ level [14]. On the other hand, higher field absorption located at ~3061 G is due to exchange coupled pairs or large Cr^{3+} clusters [14, 17, 23]. The last resonance at ~3571 G (g = 1.93) confirms the presence of Cr^{5+} ions, through the identification of its charge transfer state (both naturally existing and the ones produced after the charge transfer between Cr^{6+} and O^{2-}) [1, 2, 34, 35, 39]. Notice that Cr^{5+} signal at g = 1.93 follows an unexpected behavior. Specifically, its intensity decreases with increasing the SiO_2 content in clear contrast with optical absorption data. In order to resolve this apparent conflict, the ESR spectra of Cr-free samples with SiO_2 content $x = 0$ and $x = 40$ mol% are depicted in the inset of Fig. 4. It is clear that the Si-contained sample exhibits a strong microwave absorption signal centered at ~3000 G. Therefore, the superposition of this signal with the intrinsic Cr^{5+} resonance is responsible for the inverted behaviour.

Finally, in the presence of lower symmetry field component and spin-orbit coupling, the degeneracy of the spin states is lifted up into two Kramer's doublets with the observed resonances of g values at 2.25 and 1.93. The signal obtained at g = 4.82 refers to isolated Cr^{3+} ions within the glass

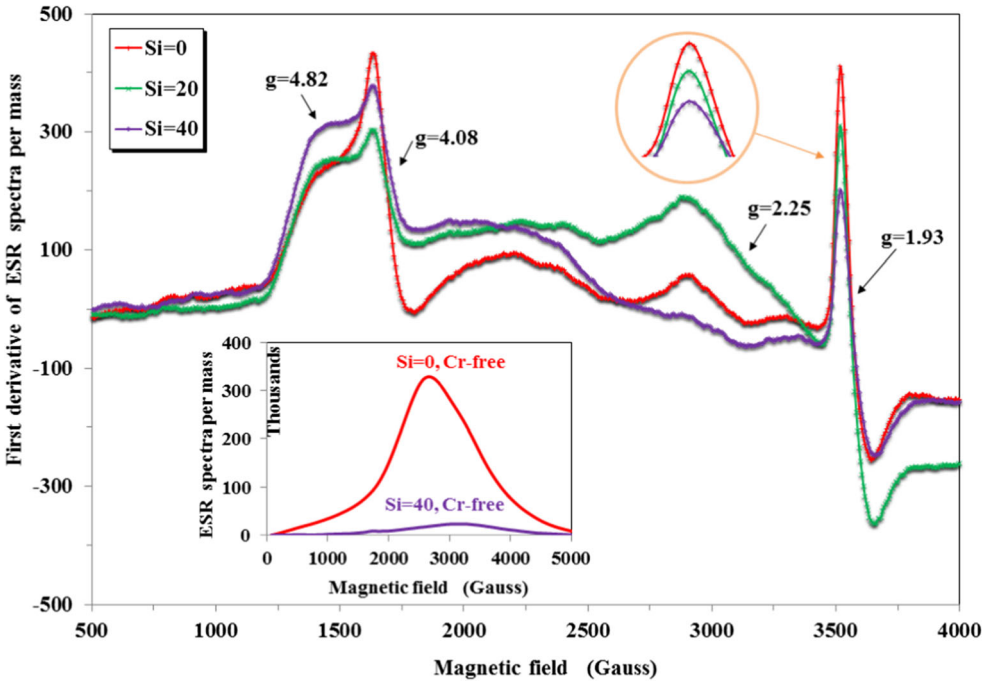

Fig. 4 ESR spectra for selected glass samples (x = 0, 20 and 40 mol%), the inset figure shows the ESR signal of the Cr-free of Si = 0 and Si = 40 samples

network, while the intense signal at g = 4.08 arises due to magnetic exchange coupling between Cr^{3+} and Cr^{3+} ion pairs [14, 22, 25, 36].

3.4 FTIR Results

The FTIR absorption spectra of the prepared samples are shown in Fig. 5. The SiO_2-free sample is characterized by broad bands with complex features which are mainly consisting of vibrational bands from combined BO_3 and BO_4 structural units, in addition to a weak low energy resonance originating from the modifier and TM-dopant (Li and Cr ions) [46–49]. The main absorption bands are centered at 690 cm^{-1} (is generated by the B-O-B bending vibrations of BO_3 units), 960 cm^{-1} (could be attributed to B-O asymmetric stretching of tetrahedral BO_4 groups) and 1380 cm^{-1} (is assigned to the stretching vibrationsof the BO_3 triangles) [46–49]. While the modifier band is found at wavenumbers

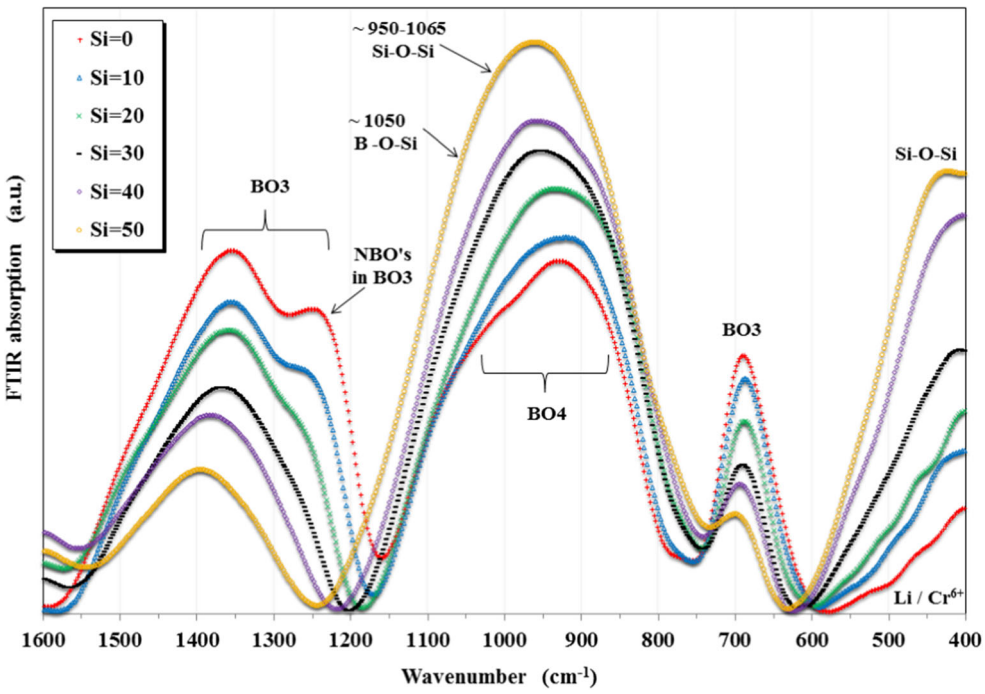

Fig. 5 FTIR spectra of all prepared samples

less than 600 cm^{-1}, for the lithium containing glasses the weak band at (439–470) cm^{-1} is due to Li ionic vibrational units [2, 50], and rather likely overlaps with Cr^{6+} band [1, 2, 12]. When doped with SiO_2, a number of drastic changes in intensity and band position take place for all those vibrational modes. Specifically, the modifier band observed below 600 cm^{-1} gains intensity, after SiO_2 doping, resulting from Si–O–Si bending modes of bridging oxygen's [49, 51, 52]. Likewise, the BO_4 band shows higher intensity due to the formation of Si-O-Si and B-O-Si bonds which contribute vibrational modes at 950–1065 and ~ 1050 cm^{-1}, respectively. These linkages were combined with the band B–O–B tetrahedral structural with increasing SiO_2 in the glass network. All FTIR bands are shifted towards higher wavenumber with increasing the concentration of SiO_2 [2, 53]. In contrast to BO_4 and modifier bands, the BO_3 bands at 690 and 1380 cm^{-1} are significantly reduced. This is a clear indication of the fact that BO_3 borate groups and NBOs are decreasing in the glass structure [49, 52]. Of particular importance, is the behaviour of the shoulder around 1240 cm^{-1} which is due to B-O asymmetric band and reflects the number of non-bridging oxygens (NBOs) of BO_3triangles [1, 54, 55]. This shoulder exhibits dramatic intensity reduction until it eventually vanishes for the highest SiO_2 concentration here explored. Such a less NBO's structure might be attributed to the decreases in the degree of localization of electrons and donor centers lead to large energy gaps confirming the optical absorption results [42, 49, 56].

4 Conclusion

The optical transitions of Cr ions in borosilicate glass system of composition $xSiO_2$- (75-x) B_2O_3–24.7Li_2O-0.3Cr_2O_3 (x = 0, 10, 20, 30, 40 and 50 mol%) were investigated. The addition of silicon oxide on borate glasses enhanced their amorphous nature and simultaneously produced suitable modification in Cr^{3+} and Cr^{6+} optical transitions (i.e., promotes the formation of Cr^{6+} in the glassy samples). It was noted that the replacement of Boron oxide by Silicon oxide influences the ESR spectra rather clearly. Indeed, SiO_2 absorbs significant portion of the microwave responsible for the spin transition mechanism, leading to an opposite behavior for the intensity of the transformed Cr^{6+} band (i.e. Cr^{5+}). The present compositions stand as good candidates for multifunction optical applications such as optical switches and UV-filters.

References

1. Moukhtar A Hassan, FM Ebrahim, MG Moustafa, ZM Abd El-Fattah, MM El-Okr, J (2019) Non Cryst. Solids515 157
2. Hassan MA, Ahmad F, Abd El-Fattah ZM (2018) Novel identification of ultraviolet/visible Cr6+/Cr3+ optical transitions in borate glasses. J Alloys Compd 750:320–327
3. Ahmad F, Nabhan E (2019) Optical and. Quantum Electronics 51(8):261
4. A Samir, Moukhtar A Hassan, A Abokhadra, LI Soliman, M Elokr (2019). Optical and Quantum Electronics 51 123
5. Ebrahimi E, Rezvani M (2018) Spectrochim. Acta Part A Mol Biomol Spectrosc 190:534–538
6. Jia-Jun He, Shao-YiWu, Li-Juan Zhang, Yong-Qiang Xu, Chang-Chun Ding (2016). J. Non Cryst. Solids437 58
7. Wen H, Tanner PA (2015) Optical properties of 3d transition metal ion-doped sodium borosilicate glass. J Alloys Compd 625:328–335
8. Hassan MA, Farouk M, Abdullah AH, Kashef I, ElOkr MM (2012) ESR and ligand field theory studies of Nd2O3 doped borochoromate glasses. J Alloys Compd 539:233–236
9. VenkateswaraRao G, Veeraiah N (2002). J Alloys Compd 339:54
10. Suresh S, Narendrudu T, Yusub S, Suneel Kumar A, Ravi Kumar V, Veeraiah N, Krishna Rao D (2016) Spectrochim. Acta Part A Mol Biomol Spectrosc 153:281–288
11. Durga DK, Veeraiah N (2002) Physical properties of ZnF2–As2O3–TeO2 glasses doped with Cr3+ ions. Phys B 324:127–141
12. Vijay R, RameshBabu P, Ravi Kumar V, Piasecki M, KrishnaRao D, Veeraiah N (2015) Dielectric dispersion and ac conduction phenomena of Li2O−Sb2O3−PbO−GeO2:Cr2O3 glass system. Mater Sci Semicond Process 35:96–108
13. Little Flower G, Srinivasa Reddy M, SahayaBaskaran G, Veeraiah N (2007) The structural influence of chromium ions in lead gallium phosphate glasses by means of spectroscopic studies. Opt Mater 30: 357–363
14. Vijay S, Sivaramaiah G, J.L., Rao C, Kim SH (2014). Mater. Res. Bull. 60:397
15. LakshmanaRao B, Ravi YNC, Babu SVGVAP (2013). J. Non Cryst.Solids 382:99
16. Santhan Kumar J, Lakshmi Kumari J, SubbaRao M (2013) Sandhya Cole. Opt Mater 35:1320–1326
17. Ahmad F, Hassan Aly E, Atef M, ElOkr MM (2014) Study the influence of zinc oxide addition on cobalt doped alkaline earth borate glasses. J Alloys Compd 593:250–255
18. Meejitpaisan P, Kaewkhao J, Limsuwan P, Kedkaew C (2012) Physical and optical properties of the SLS glass doped with low Cr2O3 concentrations. Procedia Engineering 32:787–792
19. De Vicente FS, Santos FA, Sińes BS, Dias ST, Li MS (2014). Opt. Mater 38:119
20. Abdel-Baki M, El-Diasty F (2011) Role of oxygen on the optical properties of borate glass doped with ZnO. J Solid State Chem 184: 2762–2769
21. Dahshan A, Yasser B, Saddeek KA, Aly KHS, Shaaban MF, Husseine A, Abo El Naga SA, Shaban SO, Mahmoud J (2019). Non Cryst. Solids 508:51
22. Edukondalu A, Purnima M, Srinivasy C, Sripathi T, Awasthi AM, SyedRahman K, SivaKumar J (2012). Non Cryst. Solids 358:2581
23. Padlyak BV, Ryba-Romanowsk W, Lisiecki R, Adamiv VT, Burak YV, Teslyuk IM (2012). Opt. Mater. 34:2112
24. NagaRaju G, Veeraiah N, Nagarjuna G, Satyanarayana PVV (2006) The structural role of chromium ions on the improvement of insulating character of ZnO–ZnF2–B2O3 glass system by means of dielectric, spectroscopic and magnetic properties. Phys B 373: 297–305
25. Ahmad F (2014) Study the effect of alkali/alkaline earth addition on the environment of borochromate glasses by means of spectroscopic analysis. J Alloys Compd 586:605–610
26. Hassan MA (2013) Effect of halides addition on the ligand field of chromium in alkali borate glasses. J Alloys Compd 574:391–397
27. Bahra M, Jaafar MS, H. (2018) Wagiran. J Lumin 204:375

28. Khan I, Shoaib M, Rooh G, Kaewkhao J, Khattak SA, Ahmad T, Zaman F, Ataullah MT (2019). J. Alloys Compd. 805:896
29. Fudzi FM, Kamari HM, Latif AA, Noorazlan AM (2017). J. Nanomater. 2017:4150802
30. Kaur A, Khan S, Kumar D, Bhatia V, Rao SM, Kaur N, Singh K, Kumar A, Singh SP (2020). J. Lumin. 219:116872
31. Kim SY, Park J, Kim SH, Kadathala L, Baek JH, Kim JH, Choi JH (2020). Appl. Sci. 10(1):353
32. Ahmad F, Hassan MA (2019) Structure and Physical Properties of Al2O3Nanofillers Embedded in Poly(Vinyl Alcohol). Polym Compos 40:E647–E653
33. Ravikumar RVSSN, Yamauchi J, Chandrasekhar AV, Reddy YP, SambasivaRao P (2005). J. Mol. Struct. 740:169
34. CzKoepke K, Wisniewski M, Grinberg M (2002). J Alloys Compd 341:19
35. CzKoepke K, Wisniewski M, Grinberg FR (2002). J Phys Condens Matter 14:11553
36. Giridhar G, SreehariSastry S, Rangacharyulu M (2011) Spectroscopic studies on Pb3O4–ZnO–P2O5 glasses doped with transition metal ions. Phys B 406:4027–4030
37. Kłonkowski AM, Dunajska D, Biczkowski M, Jankowska-Frydel A (2002) The coordination state and valence state of selected transition metal ions in SiO2–B2O3 xerogels. J Non-Cryst Solids 311: 10–23
38. Ravikumar RVSSN, Komatsu R, Ikeda K, Chandrasekhar AV, Reddy BJ, Reddy YP, Rao PS (2003). J. Phys. Chem. Solids 64:261
39. Kesavulu CR, Chakradhar RPS, Jayasankar CK, Lakshmana Rao J (2010) EPR, optical, photoluminescence studies of Cr3+ ions in Li2O–Cs2O–B2O3 glasses – An evidence of mixed alkali effect. J Mol Struct 975:93–99
40. SrinivasaRao P, Ramesh Babu P, Vijay R, Narendrudu T, Veeraiah N, Krishna Rao D (2014). Mater Res Bull 57:58
41. Tauc J (1974) In: Tauc J (ed) Amorphous and liquid semiconductors. Plenum, NewYork, p 171
42. Murali Krishna G, AnilaKumari B, Srinivasa Reddy M, Veeraiah N (2007) Characterization and physical properties of Li2O–CaF2–P2O5 glass ceramics with Cr2O3 as a nucleating agent—Physical properties. J Solid State Chem 180:2747–2755
43. Schneider H, Ikeda K, Saruhan B, Rager H (1996) Electron paramagnetic resonance and optical absorption studies on Cr-doped mullite precursors. J Eur Ceram Soc 16:211–215
44. Vijay S, Chakradhar RPS, J.L., Rao H-YK (2009). Solid State Sci 11:870
45. LaxmiKanth C, Raghavaiah BV, AppaRao B, Veeraiah N (2005) Spectroscopic investigations on ZnF2–MO–TeO2 (MO=ZnO, CdO and PbO) glasses doped with chromium ions. J Quant Spectrosc RadiatTransf 90:97–113
46. Yadav A, Dahiya MS (2017) A. Hooda, Prem Chand, S. Khasa. Solid State Sci 70:54–65
47. Ciceo-Lucacel R, Ardelean I (2007) FT-IR and Raman study of silver lead borate-based glasses. J Non-Cryst Solids 353:2020–2024
48. Sailaja B, Joyce Stella R, ThirumalaRao G, Jaya Raja B, PushpaManjari V, Ravikumar RVSSN (2015). J. Mol. Struct. 1096:129
49. Abd El-Fattah ZM, Ahmad F, Hassan MA (2017) Tuning the structural and optical properties in cobalt oxide-doped borosilicate glasses. J Alloys Compd 728:773–779
50. Verhoef AH, den Hartog HW (1995) Infrared spectroscopy of network and cation dynamics in binary and mixed alkali borate glasses. J Non CrystSolids 182:221–234
51. Molla AR, Kesavulu CR, Chakradhar RPS, Tarafder A, Mohanty SK, Rao JL, Karmakar B, Biswas SK (2014) Microstructure, mechanical, thermal, EPR, and optical properties of MgAl2O4:Cr3+ spinel glass–ceramic nanocomposites. J Alloys Compd 583:498–509
52. ChandkiramGautam AKY, Singh AK (2012). ISRN Ceram. 17: 428497
53. Ramesh Babu A, Yusub S, VinayaTeja PM, SrinivasaRao P, Arunaa V, Krishna Rao D (2019) Effect of Cr2O3 on the structural, optical and dielectric studies of LiF-SrO-B2O3 glasses. J Non-Cryst Solids 520:119428
54. Krogh-Moe J (1965). Phys Chem Glasses 6:46
55. Kamitsos EI, Patsis AP, Karakassides MA, Chryssikos GD, Non-Cryst J (1990). Solids 126:52
56. Mohamed EA, Ahmad F, Aly KA (2012). J Alloys Compd 538:23